

ORDER, DISORDER, AND PHASE TRANSITION
IN CONDENSED SYSTEM

Modulated Magnetic Structure in Quasi-One-Dimensional Clinopyroxene $\text{NaFeGe}_2\text{O}_6$

T. V. Drokina^{a,b,*}, G. A. Petrakovskii^{a,b}, L. Keller^c, J. Schefer^c,
A. D. Balaev^a, A. V. Kartashev^a, and D. A. Ivanov^a

^aKirensky Institute of Physics, Siberian Branch, Russian Academy of Sciences, Krasnoyarsk, 660036 Russia

* e-mail: tvd@iph.krasn.ru

^bSiberian Federal University, Krasnoyarsk, 660074 Russia

^cLaboratory for Neutron Scattering, ETH Zürich and Paul Scherrer Institut CH-5232 Villigen PSI, Switzerland

Received June 2, 2010

Abstract—The magnetic structure of the $\text{NaFeGe}_2\text{O}_6$ monoclinic compound has been experimentally investigated using the elastic scattering of neutrons. At a temperature of 1.6 K, an incommensurate magnetic structure has been observed in the form of an antiferromagnetic helix formed by a pairs of the Fe^{3+} ions with helical modulation in the ac plane of the crystal lattice. The wave vector of the magnetic structure has been determined and its temperature behavior has been studied. The analysis of the temperature dependences of the specific heat and susceptibility, as well as the isotherms of the field dependence of the magnetization, has revealed the existence of not only the order–disorder magnetic phase transition at the point $T_N = 13$ K, but also an additional magnetic phase transition at the point $T_c = 11.5$ K, which is assumingly an orientation phase transition.

DOI: 10.1134/S1063776110061093

1. INTRODUCTION

Pyroxenes characterized by the general formula ABX_2O_6 (cation A is one of uni- and bivalent metals Na, Li, and Ca; B is one of cations Mg, Cr, Cu, Ni, Co, Fe, Mn, Al, Ga, Ti, Sc, In, V, etc.; and X is cation Ge or Si) form a wide class of compounds. The investigation of these compounds is of interest primarily in view of the possibilities of, first, formation of various magnetic structures and, second, observation and investigation of the nature of the interaction between the magnetic and electric subsystems (multiferroics are promising materials for spintronics) [1–8]. These possibilities exist because the presence of competing exchange interactions was revealed in compounds with the pyroxene structure [1]. In this aspect, of special interest is the observation and investigation of modulated magnetic structures [9, 10], in particular, due to the assuming connection of their nature with the mechanism of the interaction between the magnetic and electric subsystems [3, 11].

A low magnetic dimension manifested in pyroxenes is also of interest in view of the possibility of observing quantum effects such as the singlet ground magnetic state, formation of the energy gap in the elementary excitation spectrum, and quantum contraction of the spin [12, 13].

In view of the above circumstances, the detailed investigation of the properties and magnetic structure

of pyroxenes with various compositions is of current interest.

The $\text{NaFeGe}_2\text{O}_6$ compound is a pyroxene. The X-ray diffraction investigation of $\text{NaFeGe}_2\text{O}_6$ indicates that its crystal structure is of the same type as the structure of diopside $\text{CaMgSi}_2\text{O}_6$ with the change of Ca, Mg, and Si to Na, Fe, and Ge, respectively [14]. The crystal symmetry is described by the monoclinic space group $C2/c$ [14]. The unit cell contains four formula units (see Fig. 1). According to the X-ray diffraction investigation, the parameters of the monoclinic cell of $\text{NaFeGe}_2\text{O}_6$ at room temperature are $a = 10.0100$ Å, $b = 8.9400$ Å, $c = 5.5200$ Å, and $\beta =$

Table 1. Coordinates of the basic atoms of the $\text{NaFeGe}_2\text{O}_6$ compound at $T = 300$ K [14]

Atom	x	y	z
Ge	0.2121	0.4065	0.2689
Fe	0	0.098	0.250
Na	0	0.696	0.250
O _I	0.391	0.418	0.363
O _{II}	0.145	0.228	0.197
O _{III}	0.141	0.492	0.513

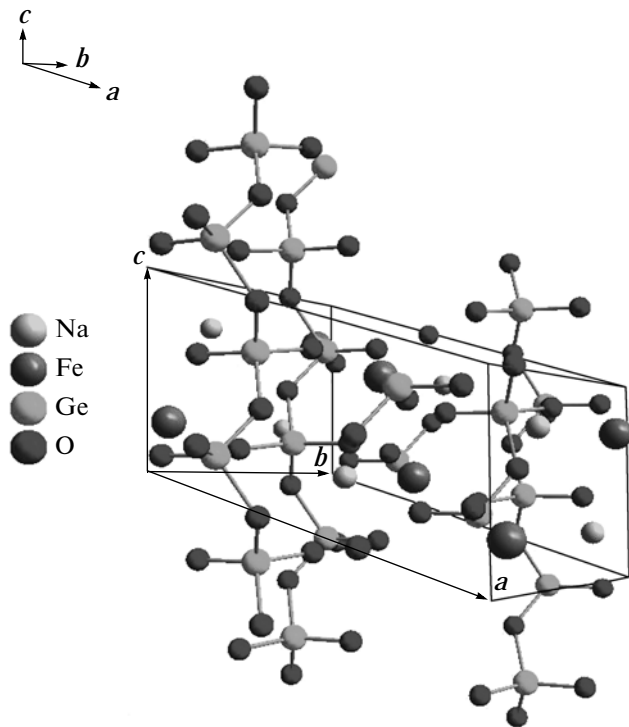


Fig. 1. Crystal structure of the $\text{NaFeGe}_2\text{O}_6$ compound in the paramagnetic region.

108.0000° [14]. The coordinates of the Na, Fe, Ge, and O ions are presented in Table 1.

Our investigations of nuclear γ -resonance performed at room temperature with a Co^{57} (Cr) source with powders 5–10 mg/cm² in thickness in terms of the natural content of iron, the Fe^{3+} ions in $\text{NaFeGe}_2\text{O}_6$ are in a high-spin state ($S = 5/2$) and in octahedral oxygen environment (the isomer shift is 0.40 mm/s), and polyhedra around the Fe atoms are distorted (the quadrupole splitting is $Q = 0.34$ mm/s) [15].

Octahedra in the crystal structure of iron-based sodium pyroxene are connected through common edges into continuous zigzag belts along the c crystal axis. The GeO_4 tetrahedra are connected with each other through vertexes and also form chains along the c axis. Two types of the chains alternate along the b crystal axis.

The SQUID magnetic measurements of the $\text{NaFeGe}_2\text{O}_6$ compounds in a magnetic field of 100 Oe indicate that $\text{NaFeGe}_2\text{O}_6$ at high temperatures ($T > 15$ K) is in a paramagnetic state characterized by the asymptotic Néel temperature $\theta = -135$ K; the inverse susceptibility above $T = 100$ K is described by the Curie–Weiss law [15]. At a temperature below 15 K, the sample transits from the paramagnetic state to the state with the long-range magnetic order formed primarily by the antiferromagnetic interaction.

The analysis of the structure features shows that two forms of the exchange interactions between nearest neighbors are possible in pyroxene $\text{NaFeGe}_2\text{O}_6$: first, interactions occurring through the Fe–O–Fe bonds and, second, interchain exchange interactions Fe–O–Ge–O–Fe both belonging to one ab layer and interlayer. The features of the topology of exchange interactions in $\text{NaFeGe}_2\text{O}_6$ and their competition can lead to the nontrivial magnetic structure of this compound. For this reason, the aim of this work is to study the magnetic structure of pyroxene $\text{NaFeGe}_2\text{O}_6$.

2. SAMPLE PREPARATION AND EXPERIMENTAL PROCEDURE

A polycrystalline $\text{NaFeGe}_2\text{O}_6$ sample was synthesized from 16% Na_2CO_3 , 23% Fe_2O_3 , and 61% GeO_2 reagents by the solid-state reaction method with annealings at temperatures of 800–900°C in air at four stages each with a duration of 24 h. The lattice parameters determined by the X-ray diffraction analysis are $a = 10.008$ Å, $b = 8.948$ Å, $c = 5.523$ Å, and $\beta = 107.59^\circ$, which are in agreement with the data reported in [14]. The X-ray diffraction pattern contains traces of the nonmagnetic impurity phase $\text{Na}_4\text{Ge}_9\text{O}_{20}$.

The elastic scattering of neutrons was used as the main method of investigations. The experiments on the scattering of neutrons with a wavelength of $\lambda = 2.4576$ Å were performed at temperatures of 1.6–100 K on a DMC diffractometer (SINQ, Switzerland) [16, 17]. The sample in the cylindrical vanadium container was placed into a helium cryostat. The data were processed using the FullProf suite [18]. To determine the magnetic structure, the necessary separation of the magnetic component from the nuclear component was performed by subtracting the diffraction pattern at a temperature of 30 K, at which the sample in the paramagnetic state, from the neutron diffraction pattern at $T = 1.6$ K.

The magnetic measurements were performed on an automated vibration magnetometer with a superconducting solenoid in fields up to 8 T at temperatures of 4.2–300 K at the Kirensky Institute of Physics, Siberian Branch, Russian Academy of Sciences, Krasnoyarsk, Russia.

The calorimetric investigations in the temperature range of 2.0–300 K in magnetic fields up to 9 T were performed using a Quantum Design PPMS 6000 instrument at Shared Usage Center, Krasnoyarsk Scientific Center.

3. EXPERIMENTAL RESULTS AND THEIR DISCUSSION

The neutron diffraction investigation of the magnetic structure of the $\text{NaFeGe}_2\text{O}_6$ polycrystal indicates that the neutron diffraction pattern below a temperature of 13 K corresponding to the transition of the

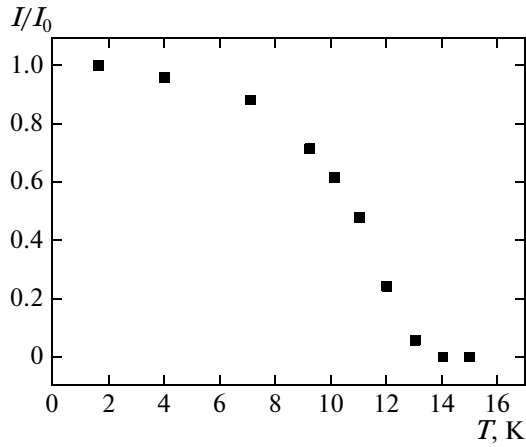


Fig. 2. Temperature dependence of the relative integral intensity of the Bragg magnetic peak $(0, 1, 0) \pm \mathbf{k}$ on the neutron diffraction pattern of the $\text{NaFeGe}_2\text{O}_6$ compound normalized to the intensity I_0 at $T = 1.6$ K. The Néel temperature is $T_N \approx 13$ K.

sample to the antiferromagnetic state contains a large number of magnetic peaks attributed to the long-range magnetic order. Figure 2 shows the temperature dependence of the height of the most intense magnetic peak $(0, 1, 0) \pm \mathbf{k}$ on the neutron diffraction pattern of the $\text{NaFeGe}_2\text{O}_6$ compound; it is seen that the long-range magnetic order appears at $T = 13$ K. This result is consistent with the SQUID magnetic measurements [15]. The integral intensity of the magnetic component of the neutron scattering decreases with an increase in the temperature. Saturation is not reached at the lowest temperature $T = 1.6$ K.

The analysis of the positions of the magnetic reflections indicates an incommensurate magnetic structure in the $\text{NaFeGe}_2\text{O}_6$ compound. The wave vector of the structure at the temperature $T = 1.6$ K is $\mathbf{k} = (0.3357(4), 0, 0.0814(3))$.

In order to determine the orientation of the magnetic moments of atoms in the magnetic structure with respect to each other and to crystallographic axes, the experimental data for $T = 1.6$ K were processed according to [18]. The simulation results indicate that

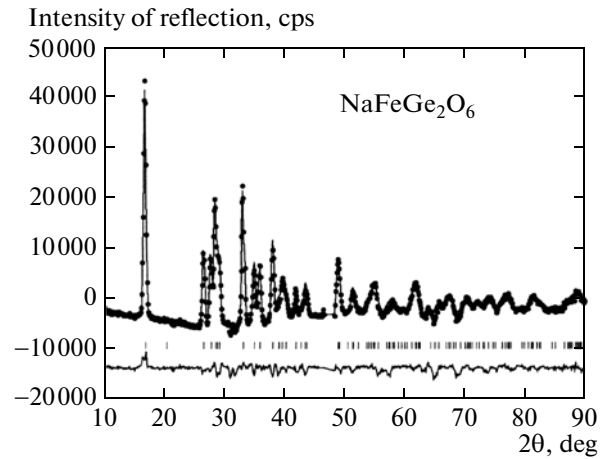


Fig. 3. (Points) Neutron diffraction pattern of the magnetic scattering of neutrons from the $\text{NaFeGe}_2\text{O}_6$ polycrystalline sample at $T = 1.6$ K obtained by taking into account the subtraction of the data at 30 K. The lines correspond to the model calculation of the reflections for the helical modulation of magnetic moments and (lower line) deviation of the experimental data from the calculation.

there are two models that can describe both the positions and intensities of the Bragg magnetic peaks on the dependence of the neutron scattering intensity on the magnetic scattering angle θ . Both models imply that the magnetic moments of iron ions in the incommensurate structure of $\text{NaFeGe}_2\text{O}_6$ form antiferromagnetically coupled pairs with modulation along the propagation vector \mathbf{k} . One model describes the sinusoidal modulation of the magnetic moments and the other, helical modulation. Table 2 presents the results of the neutron diffraction investigation of the magnetic structure in $\text{NaFeGe}_2\text{O}_6$ corresponding to the sinusoidal and helical modulations of spins. The model with helical modulation is in better agreement with the experimental data.

Figure 3 shows the neutron diffraction pattern for $T = 1.6$ K after the subtraction of the data for $T = 30$ K for the helical modulation of magnetic moments. This pattern contains only the reflections caused by the magnetic ordering of the sample. It is seen that the

Table 2. Neutron diffraction data for the magnetic structure in the $\text{NaFeGe}_2\text{O}_6$ compound at $T = 1.6$ K

Magnetic structure of the crystal	Incommensurate structure with the helical modulation of antiferromagnetically coupled pairs	Incommensurate structure with the sinusoidal modulation of antiferromagnetically coupled pairs
Propagation vector of the magnetic structure	$\mathbf{k} = (0.3357(4), 0, 0.0814(3))$	$\mathbf{k} = (0.3357(4), 0, 0.0814(3))$
Magnetic moment of the Fe^{3+} ion	$M = 2.55(1)\mu_B$	$M = 2.53(2)\mu_B$
Orientation of the magnetic moments	in the ac plane (small component along the b axis)	in the ac plane (no component along the b axis)
Reliability of the result processing factors	$R_p = 4.5, \chi^2 = 4.43$	$R_p = 6.5, \chi^2 = 13.2$

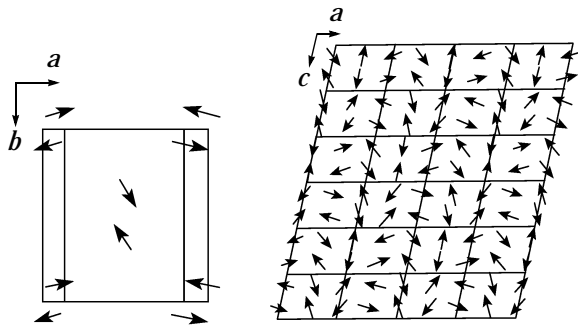


Fig. 4. Magnetic structure in $\text{NaFeGe}_2\text{O}_6$ at $T = 1.6$ K; (a) arrangement of the magnetic moments of iron in a crystal cell (view along the c axis in the ab plane) and (b) arrangement of the magnetic moments of iron in a number of crystal cells (the ac plane). The magnetic structure in $\text{NaFeGe}_2\text{O}_6$ is formed by antiferromagnetically coupled pairs of Fe^{3+} ions.

model of the magnetic structure with helical modulation is in good agreement with the experimental data including a large number of magnetic peaks throughout the magnetic scattering angle range. This means that the incommensurate magnetic structure with the helical modulation of the magnetic moments of iron ions along the propagation vector \mathbf{k} exists in the $\text{NaFeGe}_2\text{O}_6$ compound at $T = 1.6$ K magnetic scattering angle range. The magnetic moment of the Fe^{3+} ion at $T = 1.6$ K is $2.55(1)\mu_B$.

Figure 4a shows the arrangement of the magnetic moments in a unit cell. The magnetic moments of the modulated structure are located primarily in the ac plane and there is only a small component along the b axis. The magnetic structure can be represented as the long-wave modulation of the antiferromagnetic structure (see Fig. 4b).

Microscopic mechanisms responsible for the modulation of magnetic structures are mainly known [9].

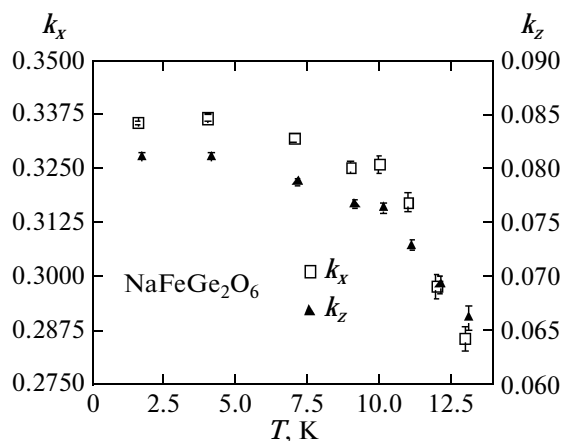


Fig. 5. Temperature dependence of the wave vector of the magnetic structure for $\text{NaFeGe}_2\text{O}_6$. The vertical error bars show the measurement errors.

The helical magnetic structure in metagermanate $\text{NaFeGe}_2\text{O}_6$ is apparently due to the “competition” between exchange interactions between different atomic neighbors in the chains of magnetoactive ions and between them. Owing to the competition between exchange interactions, the magnetic moments of Fe^{3+} ions rotate through the plane by a certain angle α (the moments in neighboring planes are antiparallel), forming the incommensurate helical magnetic structure.

The temperature behavior of the wave vector of the magnetic structure was investigated. The results are shown in Fig. 5. The wave vector depends monotonically on the temperature, having values incommensurate with the period of the crystal lattice. The wave vector decreases with an increase in the temperature. This decrease is slowed at the values $k_x \approx 0.0325$ and $k_z \approx 0.0775$ in the range $9.5 \text{ K} < T < 10.5 \text{ K}$; this slowing apparently corresponds to the lock-in effect [9].

The temperature dependence of the propagation vector implies that the modulated helical magnetic structure changes in the temperature range of slowing the variation of the wave vector.

To further study the magnetic phase transitions, the specific heat C_p of the $\text{NaFeGe}_2\text{O}_6$ was measured in the temperature range of 2.0–300 K and the magnetic field range of 0–9 T. Figure 6 shows the temperature dependence of C_p near the Néel point. The temperature dependence of the specific heat in the absence of the external magnetic field ($H = 0$) has two maxima at $T_1 = 11.5$ K and $T_2 = 13$ K. It is worth noting that the position of the first maximum in the $C_p(T)$ dependence, in contrast to the second maximum, depends

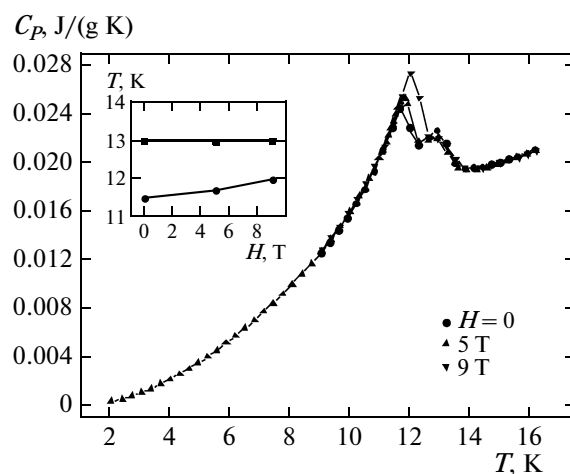


Fig. 6. Temperature dependence of the specific heat of the $\text{NaFeGe}_2\text{O}_6$ polycrystalline sample in magnetic fields $H = 0, 5,$ and 9 T. The inset shows the magnetic-field dependence of the Néel temperature T_N (■) and the spin-reorientation temperature T_c (●).

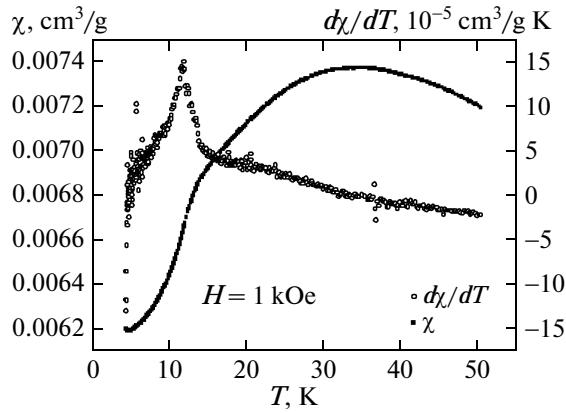


Fig. 7. Temperature dependences of the magnetic susceptibility χ and its derivative $d\chi/dT$ in $\text{NaFeGe}_2\text{O}_6$ (the maximum $d\chi/dT$ value is reached at a temperature of $T = 11.5$ K).

on the magnetic field. Its maximum shift in a field of $H = 9$ T is about 0.5 K.

In view of the features in the behavior of magnetization in $\text{NaFeGe}_2\text{O}_6$ with a decrease in the temperature [15], the maximum at T_2 on the temperature dependence of the specific heat can certainly be attributed to the order–disorder phase transition ($T_2 = T_N = 13$ K). This conclusion is also confirmed by neutron diffraction investigations (see Fig. 2). The nature of the anomaly on the $C_p(T)$ curve at $T_1 = 11.5$ K is not so obvious. Since no changes are observed in the crystal structure of the $\text{NaFeGe}_2\text{O}_6$ compounds in the low-temperature region, the phase transition at $T_1 \equiv T_c = 11.5$ K most probably corresponds to a change in the macroscopic state of the magnetic subsystem of the sample (T_c is the temperature of the reorientation of the magnetic subsystem of the sample). This assumption is confirmed by the effect of the magnetic field on the position of the low-temperature peak of the specific heat (see Fig. 6), by the pinning of the wave vector at a temperature close to T_1 (see Fig. 5), and by an anomaly on the temperature dependence of the susceptibility $\chi(T)$ (see Fig. 7). The inset in Fig. 6 shows the magnetic field dependences of the Néel temperature and the temperature of the assumed spin-reorientation transition.

The measurements of the field dependences of the susceptibility $\chi(H)$ and magnetization of the $\text{NaFeGe}_2\text{O}_6$ polycrystal at various temperatures show that a critical field H_c at which the slope of the $\chi(H)$ curve changes probably due to the reorientation of the magnetic moments exists in the magnetic ordering region at each temperature. An anomaly in the susceptibility curve $\chi(H) = d\sigma/dH$ is observed near the critical point $H_c(T)$ (see Fig. 8). This anomaly disappears when the sample was heated to a temperature of $T = 12$ K.

Using the measured magnetization and specific heat in the magnetic field, we plot the phase diagram of the magnetic state of the $\text{NaFeGe}_2\text{O}_6$ sample (see

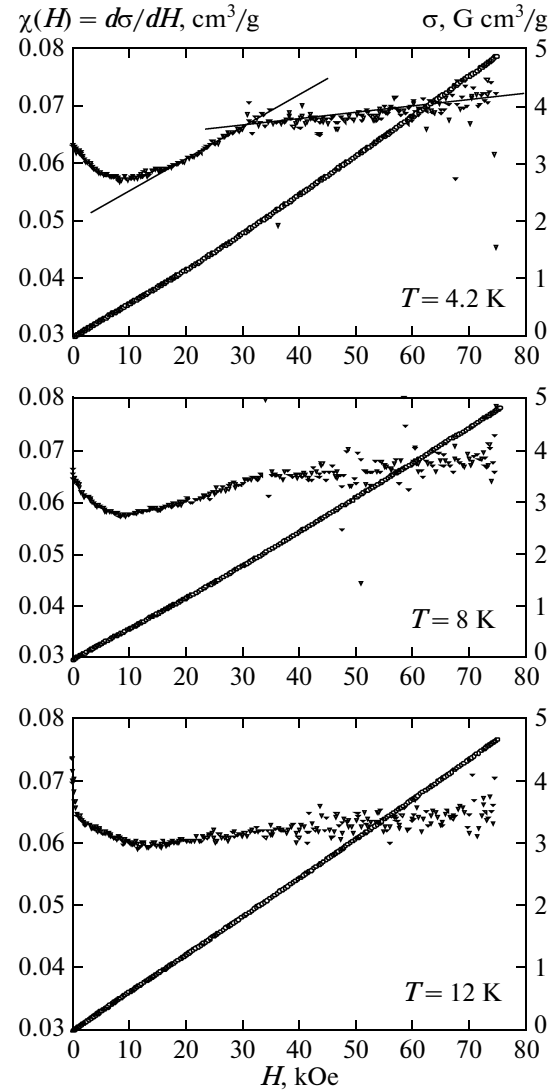


Fig. 8. Field dependences of the (∇) susceptibility and (\circ) magnetization of the $\text{NaFeGe}_2\text{O}_6$ polycrystal at temperatures $T = 4.2$ K (the critical field of the rearrangement of the magnetic subsystem of the sample is $H_c = 32$ kOe), $T = 8$ K ($H_c = 33$ kOe), and $T = 12$ K (anomaly is absent).

Fig. 9). The sample is paramagnetic in region IV. According to the investigations of the magnetization, the low-temperature helical incommensurate structure revealed by neutron-diffraction investigations in the absence of the magnetic field apparently exists throughout region II with an increase in the magnetic field. It changes in the magnetic field $H = H_c$ and another magnetic structure exists in the region of $H > H_c$ (region I). The features of the temperature dependence of the specific heat in the magnetic field (see Fig. 6) implies that the spin reorientation in metagermanate $\text{NaFeGe}_2\text{O}_6$ also occurs at temperatures above $T_c = 11.5$ K ($H = 0$) and below the order–disorder transition temperature (region III). The refinement of the picture of the magnetic order in regions I and III

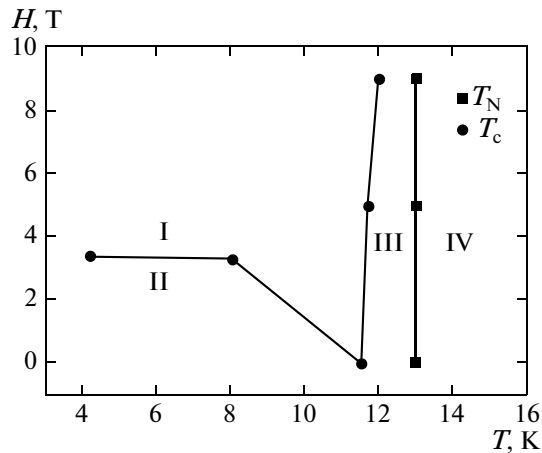


Fig. 9. Phase diagram of the magnetic state of the $\text{NaFeGe}_2\text{O}_6$ polycrystal plotted according to the measurements of the magnetization and specific heat in the magnetic field. The magnetic structure is unknown in regions I and III, is incommensurate helical magnetic structure in region II, and is paramagnetic in region IV.

and the nature of low-temperature magnetic phase transition at T_c requires additional neutron-diffraction investigations.

4. CONCLUSIONS

The magnetic structure of the $\text{NaFeGe}_2\text{O}_6$ compound has been investigated using the neutron diffraction investigations, as well as calorimetric and magnetic measurements, and magnetic phase transitions have been revealed.

The neutron diffraction pattern of the polycrystalline Na, Fe metagermanate at temperatures below $T_N = 13$ K contains additional (magnetic) peaks among the main (nuclear) reflections. The analysis of the magnetic peaks in the neutron diffraction pattern indicates that the magnetic structure formed by antiferromagnetically coupled pairs of Fe^{3+} ions with the helical modulation in the ac plane and an insignificant component along the b axis exists in the $\text{NaFeGe}_2\text{O}_6$ compound at a temperature of $T = 1.6$ K. This structure is characterized by the modulation period incommensurate with the period of the crystal lattice; in particular, the wave vector at $T = 1.6$ K is $\mathbf{k} = (0.3357(4), 0, 0.0814(3))$. With an increase in the temperature, the wave vector of the structure decreases monotonically; this monotonicity is violated in the range of $9.5 \text{ K} < T < 10.5 \text{ K}$ and the lock-in effect is observed.

The analysis of the temperature dependences of the specific heat and susceptibility, as well as the isotherms of the field dependence of the magnetization, has revealed the existence of not only the order–disorder

magnetic phase transition at the point $T_N = 13$ K, but also an additional magnetic phase transition at the point $T_c = 11.5$ K, which is assumingly an orientation phase transition.

REFERENCES

1. S. V. Streltsov and D. I. Khomskii, *Phys. Rev. B: Condens. Matter* **77**, 064405 (2008).
2. A. A. Katanin and V. Yu. Irkhin, *Usp. Fiz. Nauk* **177** (6), 639 (2007) [*Phys.—Usp.* **50** (6), 595 (2007)].
3. S. Jodlauk, P. Becker, J. A. Mydosh, D. I. Khomskii, T. Lorenz, S. V. Streltsov, D. C. Hezel, and L. Bohaty, *J. Phys.: Condens. Matter* **19**, 432201 (2007).
4. S. V. Streltsov, J. McLeod, A. Moewes, G. J. Redhammer, and E. Z. Kurmaev, *Phys. Rev. B: Condens. Matter* **81**, 045118 (2010).
5. P. J. Baker, H. J. Lewtas, S. J. Blundell, T. Lancaster, I. Franke, W. Hayes, F. L. Pratt, L. Bohaty, and P. Becker, *Phys. Rev. B: Condens. Matter* **81**, 214403 (2010).
6. G. Nenert, I. Kim, M. Isobe, C. Ritter, A. N. Vasiliev, K. H. Kim, and Y. Ueda, *Phys. Rev. B: Condens. Matter* **81**, 184408 (2010).
7. A. N. Vasiliev, O. L. Ignatchik, A. N. Sokolov, Z. Hiroi, M. Isobe, and Y. Ueda, *Phys. Rev. B: Condens. Matter* **72**, 012412 (2005).
8. M. Isobe, E. Ninomiya, A. N. Vasiliev, and Y. Ueda, *J. Phys. Soc. Jpn.* **71**, 1423 (2002).
9. Yu. A. Izyumov, *Diffraction of Neutrons on Long-Period Structures* (Energoatomizdat, Moscow, 1987) [in Russian].
10. L. E. Svistov, L. A. Prozorova, A. A. Bush, and K. E. Kamentsev, *J. Phys.: Conf. Ser.* **200**, 022062 (2010).
11. E. Golovenchits and V. Sanina, *J. Phys.: Condens. Matter* **16**, 4325 (2004).
12. V. V. Val'kov and S. G. Ovchinnikov, *Teor. Mat. Fiz.* **50** (3), 466 (1982) [*Theor. Math. Phys.* **50** (3), 306 (1982)].
13. Z. S. Popović, Ž. V. Šljivančanin, and F. R. Vukajlović, *Phys. Rev. Lett.* **93**, 036401 (2004).
14. L. P. Solov'eva and V. V. Bakakin, *Kristallografiya* **12**, 591 (1967) [*Sov. Phys. Crystallogr.* **12**, 517 (1967)].
15. T. V. Drokina, O. A. Bayukov, G. A. Petrakovskii, D. A. Velikanov, A. F. Bovina, G. N. Stepanov, and D. A. Ivanov, *Fiz. Tverd. Tela (St. Petersburg)* **50** (11), 2050 (2008) [*Phys. Solid State* **50** (11), 2141 (2008)].
16. P. Fischer, L. Keller, J. Schefer, and J. Kohlbrecher, *Neutron News* **11**, 19 (2000).
17. W. E. Fischer, *Physica B (Amsterdam)* **234–236**, 1202 (1997).
18. J. Rodriguez-Cravajal, *Physica B (Amsterdam)* **192**, 55 (1993).

Translated by R. Tyapaev